

Branching fractions and direct CP asymmetries of charmless B decay modes at the Tevatron

M. Morello^a

On behalf of the CDF Collaboration

^aScuola Normale Superiore and I.N.F.N di Pisa - Ed. C, Polo Fibonacci, Largo B. Pontecorvo, 3 - 56127 Pisa, Italy

We present new CDF results on the branching fractions and time-integrated direct CP asymmetries for B^0 and B_s^0 decay modes into pairs of charmless charged hadrons (pions or kaons). The data-set for this update amounts to 1 fb^{-1} of $\bar{p}p$ collisions at a center of mass energy 1.96 TeV. We report the first observation of the $B_s^0 \rightarrow K^- \pi^+$ mode and a measurement of its branching fraction and direct CP asymmetry. We also observe for the first time two charmless decays of the Λ_b -baryon: $\Lambda_b^0 \rightarrow p\pi^-$ and $\Lambda_b^0 \rightarrow pK^-$.

1. INTRODUCTION

The decay modes of B mesons into pairs of charmless pseudo-scalar mesons are effective probes of the quark-mixing (CKM) matrix and sensitive to potential new physics effects. The large production cross section of B hadrons of all kinds at the Tevatron allows measuring such decays in new modes, which are important to supplement our understanding of B meson decays. The still unobserved $B_s^0 \rightarrow K^- \pi^+$ mode could be used to measure γ [1] and its CP asymmetry could be a powerful model-independent test of the source of direct CP asymmetry in the B system [2]. This may provide useful information to solve the current discrepancy between the asymmetries observed in the neutral $A_{\text{CP}}(B^0 \rightarrow K^+ \pi^-)$ and charged mode $A_{\text{CP}}(B^+ \rightarrow K^+ \pi^0)$ [3].

The $B_s^0 \rightarrow \pi^+ \pi^-$ and $B^0 \rightarrow K^+ K^-$ modes proceed through annihilation and exchange topologies, which are currently poorly known and a source of significant uncertainty in many theoretical calculations [4,5]. A measurement of both modes would allow a determination of the strength of these diagrams [6].

CDF II is a multipurpose magnetic spectrometer surrounded by calorimeters and muon detectors [7]. A silicon micro-strip detector (SVXII) and a cylindrical drift chamber (COT) situated

in a 1.4 T solenoidal magnetic field reconstruct charged particles in the pseudo-rapidity range $|\eta| < 1.0$. The SVXII consists of five concentric layers of double-sided silicon detectors with radii between 2.5 and 10.6 cm, each providing a measurement with $15 \mu\text{m}$ resolution in the azimuthal (ϕ) direction and $70 \mu\text{m}$ along the beam (z) direction. The COT has 96 measurement layers, between 40 and 137 cm in radius, organized into alternating axial and $\pm 2^\circ$ stereo “super-layers”. The transverse momentum resolution is $\sigma_{p_T}/p_T \simeq 0.15\% p_T/(\text{GeV}/c)$ and the observed mass-widths are about $14 \text{ MeV}/c^2$ for $J/\psi \rightarrow \mu^+ \mu^-$ decays, and about $9 \text{ MeV}/c^2$ for $D^0 \rightarrow K^- \pi^+$ decays. The specific energy loss by ionization (dE/dx) of charged particles in the COT can be measured from the amount of charge collected by each wire.

Throughout this paper, C-conjugate modes are implied and branching fractions indicate CP-averages unless otherwise stated.

2. DATA SAMPLE

We analysed an integrated luminosity $\int \mathcal{L} dt \simeq 1 \text{ fb}^{-1}$ sample of pairs of oppositely-charged particles with $p_T > 2 \text{ GeV}/c$ and $p_T(1) + p_T(2) > 5.5 \text{ GeV}/c$, used to form $B_{(s)}^0$ meson candidates. The trigger required also a transverse opening angle $20^\circ < \Delta\phi < 135^\circ$ between the two tracks,

to reject background from particle pairs within the same jet and from back-to-back jets. In addition, both charged particles were required to originate from a displaced vertex with a large impact parameter d_0 ($100 \mu\text{m} < d_0 < 1 \text{mm}$), while the $B_{(s)}^0$ meson candidate was required to be produced in the primary $\bar{p}p$ interaction ($d_0(B) < 140 \mu\text{m}$) and to have travelled a transverse distance $L_{xy}(B) > 200 \mu\text{m}$.

In the offline analysis, an unbiased optimization procedure determined a tightened selection on track-pairs fit to a common decay vertex. We chose the selection cuts minimizing directly the expected uncertainty of the physics observables to be measured (through several ‘‘pseudo-experiments’’). We used just two different sets of cuts, respectively optimized to measure the CP asymmetry $A_{\text{CP}}(B^0 \rightarrow K^+\pi^-)$ and the branching fraction $\mathcal{B}(B_s^0 \rightarrow K^-\pi^+)$, since those two measurements are the main focus of the analysis. For the latter, the sensitivity for discovery and limit setting [8] was optimized rather than the statistical uncertainty on the particular parameter, since the mode had not yet been observed. It was verified that the former set of cuts is also adequate to measure other decay rates of the larger yield modes ($B^0 \rightarrow \pi^+\pi^-$, $B_s^0 \rightarrow K^+K^-$), while the latter, tighter set of cuts, is well suited to measure the decay rates and CP asymmetries related to rare modes ($B_s^0 \rightarrow \pi^+\pi^-$, $B^0 \rightarrow K^+K^-$, $\Lambda_b^0 \rightarrow p\pi^-$ and $\Lambda_b^0 \rightarrow pK^-$).

In addition to tightening the trigger cuts, in the offline analysis the discriminating power of the $B_{(s)}^0$ meson isolation and of the information provided by the 3D reconstruction capability of the CDF tracking were used, allowing a great improvement in the signal purity. Isolation is defined as $I(B) = p_{\text{T}}(B)/[p_{\text{T}}(B) + \sum_i p_{\text{T}}(i)]$, in which the sum runs over every other track (not from the B meson) within a cone of unit radius in the $\eta - \phi$ space around the $B_{(s)}^0$ meson flight direction. By requiring $I(B) > 0.5$, we reduced the background by a factor four while keeping almost 80% of signal. The 3D silicon tracking allowed multiple vertices to be resolved along the beam direction and the rejection of fake tracks, reducing the background by a factor of two, with

only a small efficiency loss on signal. The resulting $\pi\pi$ -mass distributions (see Fig. 1) show a clean signal of $B_{(s)}^0 \rightarrow h^+h'^-$ decays. In spite of a good mass resolution ($\approx 22 \text{MeV}/c^2$), the various $B_{(s)}^0 \rightarrow h^+h'^-$ modes overlap into an unresolved mass peak.

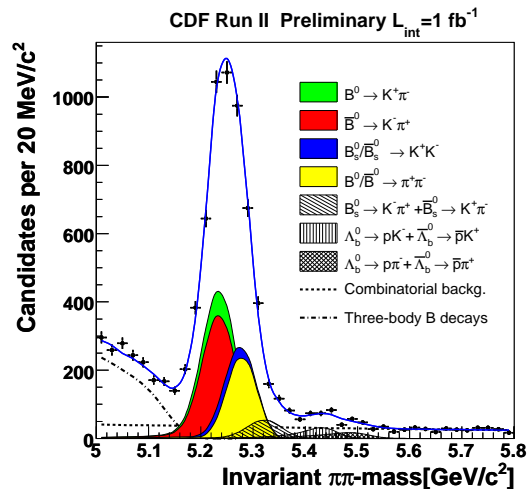


Figure 1. Invariant mass distribution of $B_{(s)}^0 \rightarrow h^+h'^-$ candidates passing all selection requirements optimized to measure $\mathcal{B}(B_s^0 \rightarrow K^-\pi^+)$, using a pion mass assumption for both decay products. Cumulative projections of the likelihood fit for each mode are overlaid.

3. FIT TO THE B DECAY-MODE COMPOSITION

The resolution in invariant mass and in particle identification is not sufficient for separating the individual decay modes on an event-by-event basis, therefore we performed an unbinned maximum likelihood fit, combining kinematic and particle identification information to statistically determine both the contribution of each mode, and the relative contributions to the CP asymmetries. For the kinematic portion, we used three

loosely correlated observables to summarize the information carried by all possible values of invariant mass of the B candidate, resulting from different mass assignments to the two outgoing particles [9]. They are: (a) the mass $M_{\pi\pi}$ calculated with the charged pion mass assignment to both particles; (b) the signed momentum imbalance $\alpha = (1 - p_1/p_2)q_1$, where p_1 (p_2) is the lower (higher) of the particle momenta, and q_1 is the sign of the charge of the particle of momentum p_1 ; (c) the scalar sum of the particle momenta $p_{tot} = p_1 + p_2$. Using these three variables, the mass of any particular mode M_{12} can be written as:

$$M_{12}^2 = M_{\pi\pi}^2 - 2m_\pi^2 + (m_1^2 + m_2^2) - 2\sqrt{p_1^2 + m_\pi^2} \cdot \sqrt{p_2^2 + m_\pi^2} - 2\sqrt{p_1^2 + m_1^2} \cdot \sqrt{p_2^2 + m_2^2}, \quad (1)$$

$$p_1 = \frac{1 - |\alpha|}{2 - |\alpha|} p_{tot}, \quad p_2 = \frac{1}{2 - |\alpha|} p_{tot}, \quad (2)$$

where m_1 (m_2) is the mass of the lower (higher) momentum particle. For simplicity, Eq. (1) is written as a function of p_1 and p_2 , but in the likelihood it was used as a function of α and p_{tot} . The simulated average values of $M_{\pi\pi}$ as a function of α for the eight $B_s^0 \rightarrow h^+h'^-$ and $\Lambda_b^0 \rightarrow ph^-$ modes are shown in Fig. 2.

Particle identification (PID) information is summarized by a single observable $\kappa_{1(2)}$ for track 1(2), defined as $\frac{dE/dx_{1(2)} - dE/dx_{1(2)}(\pi)}{dE/dx_{1(2)}(K) - dE/dx_{1(2)}(\pi)}$, where $dE/dx_{1(2)}(\pi)$ and $dE/dx_{1(2)}(K)$ are the expected $dE/dx_{1(2)}$ depositions for those particle assignments. With the chosen observables, the likelihood contribution of the i^{th} event is written as:

$$\mathcal{L}_i = (1 - b) \sum_j f_j \mathcal{L}_j^{\text{kin}} \mathcal{L}_j^{\text{PID}} + b (f_A \mathcal{L}_A^{\text{kin}} \mathcal{L}_A^{\text{PID}} + (1 - f_A) \mathcal{L}_E^{\text{kin}} \mathcal{L}_E^{\text{PID}}) \quad (3)$$

where:

$$\mathcal{L}_j^{\text{kin}} = R(M_{\pi\pi}|\alpha, p_{tot}) P_j(\alpha, p_{tot}), \quad (4)$$

$$\mathcal{L}_A^{\text{kin}} = A(M_{\pi\pi}; c_2, m_0) P_A(\alpha, p_{tot}), \quad (5)$$

$$\mathcal{L}_E^{\text{kin}} = e^{c_1 M_{\pi\pi}} P_E(\alpha, p_{tot}), \quad (6)$$

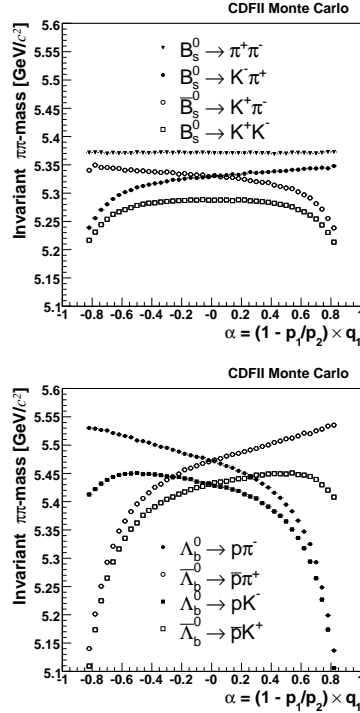


Figure 2. Average $M_{\pi\pi}$ versus α for simulated samples of B_s^0 (top) and Λ_b^0 (bottom) candidates. The corresponding plots for the B^0 are similar to B_s^0 but shifted for the mass difference.

$$\mathcal{L}_j^{\text{PID}} = F_j(\kappa_1, \kappa_2|\alpha, p_{tot}), \quad (7)$$

$$\mathcal{L}_{A(E)}^{\text{PID}} = \sum_{l,m=e,\pi,K,p} w_l^{\text{A(E)}} w_m^{\text{A(E)}} F_{lm}(\kappa_1, \kappa_2|\alpha, p_{tot}). \quad (8)$$

The various terms of the likelihood functions are described below.

The index j runs over the twelve distinguishable $B_{(s)}^0 \rightarrow h^+h'^-$ and $\Lambda_b^0 \rightarrow ph^-$ modes, and f_j are their fractions to be determined by the fit, together with the total background fraction b . The background is composed of two different kinds: combinatorial background and partially-reconstructed heavy flavor decays. The combinatorial background is composed of random pairs of charged particle, displaced from the beam-

line, accidentally satisfying the selection requirements, while the latter, referred as “physics” background, is composed of multi-body b -hadron decays (i.e. $B_{(s)}^0 \rightarrow \rho\pi/\rho K$) in which only two tracks are reconstructed. The indices A(E) label the physics (combinatorial) background quantities. The fraction of the physics background is given by f_A and it is a free parameter in the fit.

Each likelihood term, both for signals and backgrounds, is factorized into three different contributions: a) the conditional probability distribution of the invariant mass $M_{\pi\pi}$ given α and p_{tot} (for the background $M_{\pi\pi}$ is assumed to be independent of momentum), b) the joint conditional probability of PID variables κ_1, κ_2 given α, p_{tot} for a determined particles hypothesis, j in the case of signals (F_j) and l, m in the case of background ($F_{l,m}$), and c) the joint probability distribution of momentum variables α and p_{tot} ($P_{j(A,E)}$).

$R(M_{\pi\pi}|\alpha, p_{tot}) = R(M_{\pi\pi} - \mathcal{M}_j(\alpha, p_{tot}), \alpha, p_{tot})$ is the mass resolution function of each mode j when the correct mass is assigned to both tracks. The average mass $\mathcal{M}_j(\alpha, p_{tot})$ is the value of $M_{\pi\pi}$ obtained from Eq. (1) by setting the appropriate particle masses for each decay mode j and, by making a simple variable change, we obtain $R(M_{\pi\pi} - \mathcal{M}_j(\alpha, p_{tot}), \alpha, p_{tot}) = R(M_j - M_{B^0(B_s^0, \Lambda_b^0)}, \alpha, p_{tot})$, where M_j is the invariant mass computed with the correct mass assignment to both particles for each mode j . α and p_{tot} appear explicitly in the last equation since they are useful to parameterize the dependence of the mass resolution by the momenta.

The mass distribution of the physics background is parameterized with an “Argus function”, defined by the notation $A(M_{\pi\pi}; c_2, m_0)$ [10], convoluted with a Gaussian distribution centered at zero with a width, in this case, equal to the mass resolution, while the combinatorial background with an exponential function. The background mass distribution was determined in the fit by varying the parameters c_1, c_2 and m_0 in Eq. (5,6). The function $P_{j(A,E)}(\alpha, p_{tot})$ was parameterized by a product of polynomial and exponential functions fitted to Monte Carlo samples produced by a detailed de-

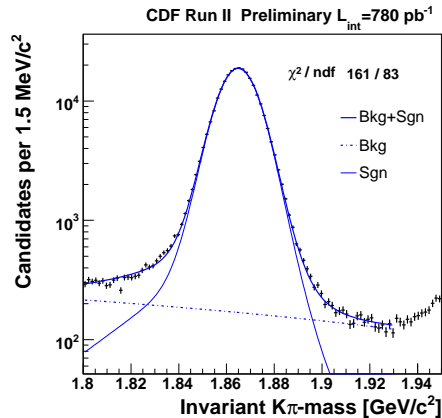


Figure 3. Tagged $D^0 \rightarrow K^- \pi^+$ decays from $D^{*+} \rightarrow D^0 \pi^+ \rightarrow [K^- \pi^+] \pi^+$: a verification of the mass line shape by performing a 1-D binned fit where the signal mass line shape is completely fixed from the model (see text).

tector simulation for each mode j , instead for the background terms was obtained from the mass sidebands of data.

The mass resolution function R was parameterized using the detailed detector simulation. To take into account non-Gaussian tails due to the emission of photons in the final state, we included soft photon emission in the simulation, using recent QED calculations [11]. The quality of the mass resolution model was verified in the simulation using about 500k $D^0 \rightarrow K^- \pi^+$ decays (see Fig. 3). The mass line-shape of the $D^0 \rightarrow K^- \pi^+$ was fitted by fixing the signal shape from the model, and allowing to vary only the background function. Good agreement was obtained between data and simulation. In Eq. (4), the nominal B^0, B_s^0 and Λ_b^0 masses measured by CDF [12] were used to reduce the systematic uncertainties related to the knowledge of the global mass scale.

A sample of 1.5M $D^{*+} \rightarrow D^0 \pi^+ \rightarrow [K^- \pi^+] \pi^+$ decays, where the D^0 decay products are identified by the charge of the D^{*+} pion, was used to calibrate the dE/dx response over the tracking volume and over time, and to determine the

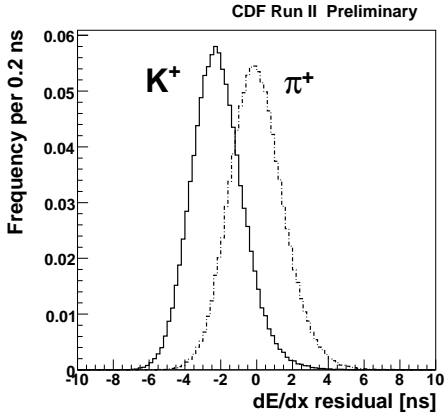


Figure 4. Tagged $D^0 \rightarrow K^-\pi^+$ decays from $D^{*+} \rightarrow D^0\pi^+ \rightarrow [K^-\pi^+]\pi^+$: distribution of dE/dx around the average pion response, for calibration samples of kaons and pions. COT samples the amount of ionization charge produced by a track by measuring the time-over-threshold (ns) of the pulse on each wire associated to the track.

$F_{j(l,m)}(\kappa_1, \kappa_2|\alpha, p_{tot})$ functions in Eq. (7,8). In a $> 95\%$ pure D^0 sample, we obtained 1.4σ separation between kaons and pions (see Fig. 4). The PID background term in Eq. (8) is similar to the signal terms, but allows for independent pion, kaon, proton, and electron components, which are free to vary independently for physics (combinatorial) background. In Eq. (8) the indices l and m run over the four possible particles e, π, K, p and the fractions of different kind of particles $w_l^{A(E)}, w_m^{A(E)}$ are free parameters in the fit. Muons are indistinguishable from pions with the available dE/dx resolution.

4. FIT RESULTS AND SYSTEMATICS

We performed two separate fits: the first using the cuts optimized to measure the direct $A_{CP}(B^0 \rightarrow K^+\pi^-)$ and the second to measure $\mathcal{B}(B_s^0 \rightarrow K^-\pi^+)$. Significant signals are seen for $B^0 \rightarrow \pi^+\pi^-$, $B^0 \rightarrow K^+\pi^-$, and $B_s^0 \rightarrow K^+K^-$, previously observed by CDF [13]. Three

new rare modes were observed for the first time: $B_s^0 \rightarrow K^-\pi^+$, $\Lambda_b^0 \rightarrow p\pi^-$ and $\Lambda_b^0 \rightarrow pK^-$ while no evidence was obtained for $B_s^0 \rightarrow \pi^+\pi^-$ or $B^0 \rightarrow K^+K^-$.

To convert the yields returned from the fit into relative branching fractions, we applied corrections for efficiencies of trigger and offline selection requirements for different decay modes. The relative efficiency corrections between modes do not exceed 20%. Most corrections were determined from the detailed detector simulation, with some exceptions which were measured using data. A momentum-averaged relative isolation efficiency between B_s^0 and B^0 of 1.07 ± 0.11 was determined from fully-reconstructed samples of $B_s^0 \rightarrow J/\psi\phi$, $B_s^0 \rightarrow D_s^-\pi^+$, $B^0 \rightarrow J/\psi K^{*0}$, and $B^0 \rightarrow D^-\pi^+$. The lower specific ionization of kaons with respect to pions in the drift chamber is responsible for a $\simeq 5\%$ lower efficiency to reconstruct a kaon. This effect was measured in a sample of $D^+ \rightarrow K^-\pi^+\pi^+$ decays triggered on two tracks, using the unbiased third track. The only correction needed for the direct CP asymmetries $A_{CP}(B^0 \rightarrow K^+\pi^-)$ and $A_{CP}(B_s^0 \rightarrow K^-\pi^+)$ was a $\leq 0.6\%$ shift due to the different probability for K^+ and K^- to interact with the tracker material. The measurement of this correction has been achieved using a sample of 1M of prompt $D^0 \rightarrow K^-\pi^+$ decays reconstructed and selected using the same criteria as $B_{(s)}^0 \rightarrow h^+h'^-$ decays. Assuming the Standard Model expectation of $A_{CP}(D^0 \rightarrow K^-\pi^+) = 0$, the difference between the number of reconstructed $D^0 \rightarrow K^-\pi^+$ and $\bar{D}^0 \rightarrow K^+\pi^-$ provides a measurement of the detector-induced asymmetry between $K^+\pi^-$ and $K^-\pi^+$ final states. Since the same fit technique developed for the $B_{(s)}^0 \rightarrow h^+h'^-$ decays was used, this measurement provides also a robust check on all possible charge asymmetry biases of the detector and dE/dx parameterizations.

The $B_s^0 \rightarrow K^+K^-$ and $B_s^0 \rightarrow \pi^+\pi^-$ modes required a special treatment, since they contain a superposition of the flavor eigenstates of the B_s^0 . Their time evolution might differ from the one of the flavor-specific modes if the width difference $\Delta\Gamma_s$ between the B_s^0 mass eigenstates is significant. The current result was derived under the assumption that both modes are dominated

Table 1

Results on data sample optimized to measure $A_{\text{CP}}(B^0 \rightarrow K^+\pi^-)$ (top) and $\mathcal{B}(B_s^0 \rightarrow K^-\pi^+)$ (bottom). Absolute branching fractions are normalized to the world-average values $\mathcal{B}(B^0 \rightarrow K^+\pi^-) = (19.7 \pm 0.6) \times 10^{-6}$ and $f_s = (10.4 \pm 1.4)\%$ and $f_d = (39.8 \pm 1.0)\%$ [3]. The first quoted uncertainty is statistical, the second is systematic. N_s is the number of fitted events for each mode. For rare modes both systematic and statistical uncertainty on N_s was quoted while for abundant modes only statistical one. For the Λ_b^0 modes only the ratio $\frac{\mathcal{B}(\Lambda_b^0 \rightarrow p\pi^-)}{\mathcal{B}(\Lambda_b^0 \rightarrow pK^-)}$ was measured.

Mode	N_s	Quantity	Measurement	$\mathcal{B}(10^{-6})$
$B^0 \rightarrow K^+\pi^-$	4045 ± 84	$\frac{\mathcal{B}(\overline{B}^0 \rightarrow K^-\pi^+) - \mathcal{B}(B^0 \rightarrow K^+\pi^-)}{\mathcal{B}(\overline{B}^0 \rightarrow K^-\pi^+) + \mathcal{B}(B^0 \rightarrow K^+\pi^-)}$	$-0.086 \pm 0.023 \pm 0.009$	
$B^0 \rightarrow \pi^+\pi^-$	1121 ± 63	$\frac{\mathcal{B}(B^0 \rightarrow \pi^+\pi^-)}{\mathcal{B}(B^0 \rightarrow K^+\pi^-)}$	$0.259 \pm 0.017 \pm 0.016$	$5.10 \pm 0.33 \pm 0.36$
$B_s^0 \rightarrow K^+K^-$	1307 ± 64	$\frac{f_s \mathcal{B}(B_s^0 \rightarrow K^+K^-)}{f_d \mathcal{B}(B^0 \rightarrow K^+\pi^-)}$	$0.324 \pm 0.019 \pm 0.041$	$24.4 \pm 1.4 \pm 4.6$
$B_s^0 \rightarrow K^-\pi^+$	$230 \pm 34 \pm 16$	$\frac{f_s \mathcal{B}(B_s^0 \rightarrow K^-\pi^+)}{f_d \mathcal{B}(B^0 \rightarrow K^+\pi^-)}$	$0.066 \pm 0.010 \pm 0.010$	$5.0 \pm 0.75 \pm 1.0$
		$\frac{\mathcal{B}(\overline{B}_s^0 \rightarrow K^+\pi^-) - \mathcal{B}(B_s^0 \rightarrow K^-\pi^+)}{\mathcal{B}(\overline{B}_s^0 \rightarrow K^+\pi^-) + \mathcal{B}(B_s^0 \rightarrow K^-\pi^+)}$	$0.39 \pm 0.15 \pm 0.08$	
		$\frac{f_d \Gamma(\overline{B}^0 \rightarrow K^-\pi^+) - \Gamma(B^0 \rightarrow K^+\pi^-)}{f_s \Gamma(\overline{B}_s^0 \rightarrow K^+\pi^-) - \Gamma(B_s^0 \rightarrow K^-\pi^+)}$	$-3.21 \pm 1.60 \pm 0.39$	
$B_s^0 \rightarrow \pi^+\pi^-$	$26 \pm 16 \pm 14$	$\frac{f_s \mathcal{B}(B_s^0 \rightarrow \pi^+\pi^-)}{f_d \mathcal{B}(B^0 \rightarrow K^+\pi^-)}$	$0.007 \pm 0.004 \pm 0.005$	$0.53 \pm 0.31 \pm 0.40$ (< 1.36 @ 90% CL)
$B^0 \rightarrow K^+K^-$	$61 \pm 25 \pm 35$	$\frac{\mathcal{B}(B^0 \rightarrow K^+K^-)}{\mathcal{B}(B^0 \rightarrow K^+\pi^-)}$	$0.020 \pm 0.008 \pm 0.006$	$0.39 \pm 0.16 \pm 0.12$ (< 0.7 @ 90% CL)
$\Lambda_b^0 \rightarrow pK^-$	$156 \pm 20 \pm 11$	$\frac{\mathcal{B}(\Lambda_b^0 \rightarrow p\pi^-)}{\mathcal{B}(\Lambda_b^0 \rightarrow pK^-)}$	$0.66 \pm 0.14 \pm 0.08$	
$\Lambda_b^0 \rightarrow p\pi^-$	$110 \pm 18 \pm 16$			

by the short-lived B_s^0 component, that $\Gamma_s = \Gamma_d$, and $\Delta\Gamma_s/\Gamma_s = 0.12 \pm 0.06$ [14,15]. The latter uncertainty is included in estimating the overall systematic uncertainty.

The dominant contributions to the systematic uncertainty are the statistical uncertainty on the isolation efficiency (B_s^0 modes), the uncertainty on the dE/dx calibration and parameterization, and the uncertainty of the combinatorial background model. The first is the larger systematic of all measurements with a B_s^0 meson decay (except for $A_{\text{CP}}(B_s^0 \rightarrow K^-\pi^+)$). The second systematic, due to dE/dx, is a large systematic of all measurements, although the parameterization of the dE/dx is very accurate. The fit of composition is very sensitive to the PID information. The third one is due to the statistical uncertainty of the possible combinatorial background models and it is a dominant systematic for the observables of the rare modes. Smaller systematic uncertainties are assigned for trigger efficiencies, physics background shape, kinematics, B meson

masses and lifetimes.

5. RESULTS

The relative branching fractions are listed in Table 1, where f_d and f_s indicate the production fractions respectively of B^0 and B_s^0 from fragmentation of a b quark in $\bar{p}p$ collisions. An upper limit is also quoted for modes in which no significant signal is observed [16]. We also list absolute results obtained by normalizing the data to the world-average of $\mathcal{B}(B^0 \rightarrow K^+\pi^-)$ [3]. The contributions from the likelihood fit for each decay mode are shown in Fig. 1.

We report the first observation of three new rare charmless decays $B_s^0 \rightarrow K^-\pi^+$, $\Lambda_b^0 \rightarrow p\pi^-$ and $\Lambda_b^0 \rightarrow pK^-$ with a significance respectively of 8.2σ , 6.0σ and 11.5σ . The significance includes both statistical and systematic uncertainty. The statistical uncertainty to evaluate the significance was estimated using several pseudo-experiments with no contributions from rare signals.

The branching fraction of the newly observed

mode $\mathcal{B}(B_s^0 \rightarrow K^- \pi^+) = (5.0 \pm 0.75 \pm 1.0) \times 10^{-6}$ is in agreement with the latest theoretical expectation [17] which is lower than the previous predictions [4,18]. We measured for the first time in the B_s^0 meson system the direct CP asymmetry of $A_{\text{CP}}(B_s^0 \rightarrow K^- \pi^+) = 0.39 \pm 0.15 \pm 0.08$. This value favors a large CP violation in B_s^0 meson decays, conversely it is also compatible with zero. In Ref. [2] a robust test of the Standard Model or a probe of new physics is suggested by comparison of the direct CP asymmetries in $B_s^0 \rightarrow K^- \pi^+$ and $B^0 \rightarrow K^+ \pi^-$ decays. Using HFAG input [3] we measure $\frac{\Gamma(\overline{B}^0 \rightarrow K^- \pi^+) - \Gamma(B^0 \rightarrow K^+ \pi^-)}{\Gamma(B_s^0 \rightarrow K^- \pi^+) - \Gamma(\overline{B}_s^0 \rightarrow K^+ \pi^-)} = 0.84 \pm 0.42 \pm 0.15$ where Γ is the decay width, in agreement with the Standard Model expectation of unity. Assuming that the relationship above is unity and using as input the $\mathcal{B}(B_s^0 \rightarrow K^- \pi^+)$ measured here, the world average for $A_{\text{CP}}(B^0 \rightarrow K^+ \pi^-)$ and $\mathcal{B}(B^0 \rightarrow K^+ \pi^-)$ [3], we can estimate the expected value for $A_{\text{CP}}(B_s^0 \rightarrow K^- \pi^+) \approx 0.37$ in agreement with our measurement.

The branching fraction $\mathcal{B}(B_s^0 \rightarrow K^+ K^-) = (24.4 \pm 1.4 \pm 4.6) \times 10^{-6}$ is in agreement with the latest theoretical expectation [19,20] and with the previous CDF measurement [13]. An improved systematic uncertainty is expected for the final analysis of the same sample.

The results for the B^0 are in agreement with world average values [3]. The measurement $A_{\text{CP}}(B^0 \rightarrow K^+ \pi^-) = -0.086 \pm 0.023 \pm 0.009$ is the world's second best measurement and the significance of the new world average $A_{\text{CP}}^{\text{ave}}(B^0 \rightarrow K^+ \pi^-) = -0.095 \pm 0.013$ moved from 6σ to 7σ .

The updated upper limits and the absolute branching fractions of the currently unobserved modes $B^0 \rightarrow K^+ K^-$ and $B_s^0 \rightarrow \pi^+ \pi^-$ have been reported. The rate $\mathcal{B}(B^0 \rightarrow K^+ K^-) = (0.39 \pm 0.16 \pm 0.12) \times 10^{-6}$ has the same uncertainty of the current measurements [3] while the $B_s^0 \rightarrow \pi^+ \pi^-$ upper limit (already the world's best [13]) was improved by a factor 1.3, approaching the expectations from recent calculations [5,21].

We also report the first observation of two new baryon charmless modes $\Lambda_b^0 \rightarrow p \pi^-$ and $\Lambda_b^0 \rightarrow p K^-$. We measured $\mathcal{B}(\Lambda_b^0 \rightarrow p \pi^-) / \mathcal{B}(\Lambda_b^0 \rightarrow p K^-) = 0.66 \pm 0.14 \pm 0.08$, in agreement with the expectations from [22].

REFERENCES

1. M. Gronau and J. L. Rosner, Phys. Lett. **B482** (2000) 71.
2. H. J. Lipkin, Phys. Lett. **B621** (2005) 126.
3. E. Barberio *et al.* Heavy Flavor Averaging Group (HFAG), arXiv:hep-ex/0603003.
4. M. Beneke and M. Neubert, Nucl. Phys. **B675** (2003) 333.
5. Y. D. H. Yang *et al.*, arXiv:hep-ph/0507326.
6. A. J. Buras *et al.*, Nucl. Phys. **B697** (2004) 133.
7. D. Acosta *et al.* (CDF Collaboration), Phys. Rev. **D71** (2005) 032001.
8. G. Punzi, eConf **C030908**, MODT002 (2003); arXiv:physics/0308063.
9. For a discussion of the bias in multi-component fits related to the use of multiple variables see G. Punzi, eConf **C030908**, WELT002 (2003); arXiv:physics/0401045.
10. $A(x; c_2, m_0) = \text{Norm}[x e^{-c_2(\frac{x}{m_0})^2} \sqrt{1 - (\frac{x}{m_0})^2}]$ if $x \leq m_0$, $A(x; c_2, m_0) = 0$ if $x > m_0$.
11. E. Baracchini and G. Isidori, Phys. Lett. **B633** (2006) 309.
12. D. Acosta *et al.* (CDF Collaboration), Phys. Rev. Lett. **96** (2006) 202001.
13. A. Abulencia *et al.* (CDF Collaboration), Phys. Rev. Lett. **97** (2006) 211802.
14. M. Beneke *et al.*, Phys. Lett. **B459** (1999) 631.
15. A. Lenz, arXiv:hep-ph/0412007.
16. We use frequentist limits based on Gaussian distribution of fit pulls (with systematics added in quadrature), and LR-ordering; see G. J. Feldman and R. D. Cousins, Phys. Rev. **D57** (1998) 3873.
17. A.R. Williamson, J. Zupan, Phys. Rev. **D74** (2006) 014003.
18. Xian-Qiao Yu *et al.*, Phys. Rev. **D71** (2005) 074026.
19. S. Descotes-Genon *et al.*, Phys. Rev. Lett. **97** (2006) 061801.
20. S. Baek *et al.*, arXiv:hep-ph/0610109.
21. Y. Li *et al.*, Phys. Rev. **D70** (2004) 034009.
22. R. Mohanta *et al.* Phys. Rev. **D63** (2001) 074001.